see commentary on page 565

Critical role for osteopontin in diabetic nephropathy

Susanne B. Nicholas[1,2], Joey Liu[3], Jason Kim[2], Yuelan Ren[3], Alan R. Collins[3], Lam Nguyen[2] and Willa A. Hsueh[3]

[1]Division of Nephrology, Department of Medicine, David Geffen School of Medicine at UCLA, Los Angeles, California, USA; [2]Division of Endocrinology, Department of Medicine, David Geffen School of Medicine at UCLA, Los Angeles, California, USA and [3]Division of Diabetes, Obesity and Lipids, Department of Medicine, The Methodist Hospital Research Institute, Weill Cornell School of Medicine, Houston, Texas, USA

The profibrotic adhesion molecule, osteopontin (OPN), is upregulated in kidneys of humans and mice with diabetes. The thiazolidinedione (TZD) insulin sensitizers decrease albuminuria in diabetic nephropathy (DN) and reduce OPN expression in vascular and cardiac tissue. To examine whether OPN is a critical mediator of DN we treated *db/db* mice with insulin, rosiglitazone, or pioglitazone to achieve similar fasting plasma glucose levels. The urine albumin-to-creatinine ratio and glomerular OPN expression were increased in diabetic mice, but both were reduced by the TZDs more than by insulin. We administered streptozotocin to OPN-null and OPN-wild-type mice, and OPN-null mice were bred into both type 1 ($Ins2^{akita/+}$) and 2 (*db/db*) diabetic mice. In each case, OPN deletion decreased albuminuria, mesangial area, and glomerular collagen IV, fibronectin and transforming growth factor (TGF)-β in the diabetic mice compared with their respective controls. In cultured mouse mesangial cells, TZDs but not insulin decreased angiotensin II-induced OPN expression, while recombinant OPN upregulated TGF-β, ERK/MAPK, and JNK/MAPK signaling. These studies show that OPN expression in DN mouse models enhances glomerular damage, likely through the expression of TGF-β, while its deletion protects against disease progression, suggesting that OPN might serve as a therapeutic target.

Kidney International (2010) **77,** 588–600; doi:10.1038/ki.2009.518; published online 3 February 2010

KEYWORDS: adhesion molecule; diabetic nephropathy; extracellular matrix

Correspondence: *Willa A. Hsueh, Division of Diabetes, Obesity and Lipids, Department of Medicine, The Methodist Hospital Research Institute, Weill Cornell School of Medicine, 6565 Fannin, F8-047, Houston, Texas 77030, USA. E-mail: wahsueh@tmhs.org*

Received 30 January 2009; revised 6 November 2009; accepted 10 November 2009; published online 3 February 2010

Activation of the nuclear receptor peroxisome proliferator-activated receptor-γ (PPARγ) in the kidney attenuates albuminuria in animal models of both type 1 and 2 diabetes and in humans with type 2 diabetes.[1–4] However, the mechanisms mediating these antialbuminuric effects are not known, but appear to be independent of blood glucose and blood pressure.[1,3] Recently, osteopontin (OPN), a large phosphoglycoprotein adhesion molecule, has emerged as a potentially key pathophysiologic contributor in diabetic nephropathy (DN). OPN is expressed in all glomerular cells: mesangial cells, podocytes, and endothelial cells.[5–8] Microarray analyses of diabetic versus normal kidneys identified OPN as one of the major genes upregulated in humans with DN and in mice with either type 1 diabetes induced by streptozotocin (STZ) or the type 2 *db/db* model of diabetes.[9] Ligands to PPARγ, thiazolidinediones (TZDs), suppress OPN expression in cardiomyocytes, vascular smooth muscle cells, and macrophages to attenuate cardiac fibrosis and atherosclerosis.[10,11] We, therefore, hypothesized that OPN is a critical mediator in DN and that the renal protective effect of TZDs in DN may involve suppression of OPN. To address this hypothesis, we (1) determined whether glomerular OPN expression correlated with attenuation of albuminuria in *db/db* mice treated with TZDs versus insulin, (2) defined the role of OPN in STZ-induced albuminuria using OPN knockout mice, (3) examined the effect of genetic knockout of OPN in mouse models of both type 1 and 2 diabetes, and (4) investigated OPN regulation by angiotensin II (AngII) and TZDs, and the effect of mouse recombinant OPN on transforming growth factor (TGF)-β expression and signal transduction in cultured mouse mesangial cells.

RESULTS

Thiazolidinediones improve renal changes in *db/db* mice more than insulin

Fasting plasma glucose was elevated in *db/db* mice versus *db/m* mice and remained unchanged after treatment with PPARγ ligands, rosiglitazone or pioglitazone, or with insulin for 8 weeks, similar to pretreatment levels, but progressively increased in *db/db* control mice (Table 1). Initial and final blood pressures did not change among all animal groups. Before killing, *db/db* mice weighed significantly more than

db/m mice. The ratio of body weight/tibia length was comparable in control, rosiglitazone- and pioglitazone-treated *db/m* and higher in *db/db* mice (Table 1). The ratio of kidney weight/tibia length was not different among the animals (data not shown).

Baseline albumin-to-creatinine ratio (ACR) was elevated in 8-week-old *db/db* mice (~400–700 mg/dl) and progressively increased to 1207 ± 72 μg/mg by 16 weeks, $P<0.05$, as previously reported in this model.[12] ACR in *db/m* mice (~100 mg/dl) was unchanged from initial levels (Figure 1). Insulin treatment decreased ACR in *db/db* mice to 458 ± 107 μg/mg. However, the TZDs had a greater effect to lower ACR (rosiglitazone, 217 ± 50 μg/mg; pioglitazone, 233 ± 26 μg/mg), $P<0.05$. Thus, PPARγ ligands improved ACR more than did insulin, suggesting a PPARγ effect on albumin excretion beyond the decrease in glucose.

Periodic acid Schiff (PAS) staining was performed to quantify the % mesangial area that was glomerular mesangial matrix (Figures 2a, b). There was no significant difference among the *db/m* group. However, % mesangial area was significantly higher in *db/db* control compared with insulin-treated mice, which was also significantly higher than in either rosiglitazone- or pioglitazone-treated mice. Immunohistochemistry (IHC) for glomerular fibronectin was performed to assess matrix protein accumulation. Glomerular fibronectin staining was similar to % mesangial area (Figures 2c, d) with ~6-fold increase in *db/db* control mice, a modest reduction with insulin treatment and a greater reduction by TZDs. Glomerular cores were isolated from a subset of animals to determine TGF-β protein expression. TGF-β levels were higher in *db/db* control and insulin-treated *db/db* compared with either *db/m* control or rosiglitazone-treated *db/db* mice, $P<0.05$ (Figure 2e, f).

PPARγ ligands differentially regulate glomerular OPN compared with insulin

Glomerular expression of OPN was substantially increased in *db/db* mice compared with *db/m* mice, similar to that in whole kidney of humans and animals.[9] There was a trend for insulin to decrease glomerular OPN expression after 8 weeks. In contrast, OPN expression was reduced by 40–50% in rosiglitazone- and pioglitazone-treated *db/db* mice, $P<0.05$ (Figure 3a). These observations suggested that glomerular OPN may be a potential target for PPARγ ligands, with a more modest effect of insulin.

We incubated stable mouse mesangial cells with AngII in the absence and presence of insulin, rosiglitazone, or pioglitazone to examine their direct effects on OPN expression. Quantitative reverse transcriptase-polymerase chain reaction (RT-PCR) demonstrated ~2-fold stimulation of OPN by AngII and 1.5-fold upregulation by insulin + AngII compared with untreated control cells, $P<0.05$. However, both rosiglitazone and pioglitazone downregulated OPN in the presence of AngII, to control levels, $P<0.05$. Insulin alone did not alter OPN expression in AngII-treated cells (Figure 3b).

Genetic deletion of OPN attenuates albuminuria and glomerular matrix, collagen IV, fibronectin, and TGF-β in STZ type 1 diabetes

To determine the role of OPN in DN, we induced diabetes in $OPN^{-/-}$ and $OPN^{+/+}$ control mice, on a 129 × Black Swiss background, with STZ to achieve plasma glucose levels of ~450 to 600 mg/dl compared with control mice (~100 mg/dl),

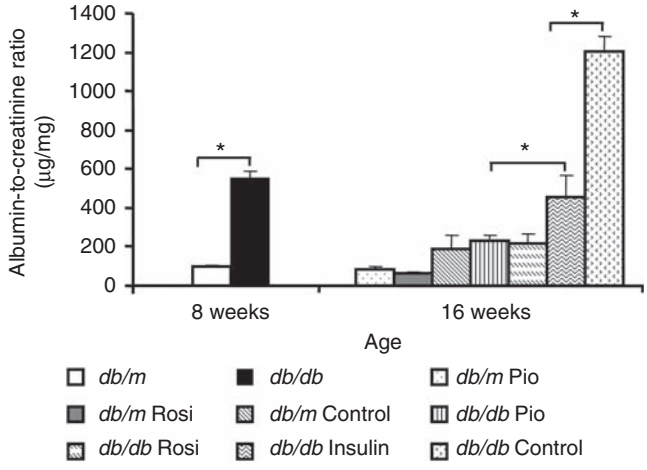

Figure 1 | PPARγ ligands improved albumin-to-creatinine ratio (ACR) more than insulin. Diabetic *db/db* and non-diabetic *db/m* mice (4–20 animals per group) were fed chow (Control) or treated with pioglitazone (Pio), rosiglitazone (Rosi) or insulin for 8 weeks. Animals were placed in metabolic cages for urine collection at age 8 weeks (initial) and at the end of the study (age 16 weeks), and albumin-to-creatinine ratio was measured, *$P<0.05$.

Table 1 | Physiological features of treated and untreated non-diabetic *db/m* and diabetic *db/db* mice

	db/m Control			*db/db* Diabetic			
	Pio	Rosi	Control	Pio	Rosi	Insulin	Control
Number of mice	6	4	8	12	8	8	20
Initial plasma glucose (mg/dl)	92 ± 4	74 ± 4	81 ± 4	271 ± 31[a]	279 ± 27[a]	299 ± 39[a]	283 ± 23[a]
Final plasma glucose (mg/dl)	134 ± 16	114 ± 15	115 ± 11	291 ± 18[a]	249 ± 22[a]	278 ± 44[a]	649 ± 17[b]
Initial SBP (mm Hg)	98 ± 7	100 ± 4	100 ± 7	92 ± 6	104 ± 3	103 ± 3	97 ± 5
Final SBP (mm Hg)	109 ± 6	100 ± 5	111 ± 3	108 ± 11	100 ± 4	98 ± 3	93 ± 3
Body weight/tibia length (g/mm)	1.4 ± 0.01	1.5 ± 0.03	1.4 ± 0.03	3.8 ± 0.09[a]	3.0 ± 0.05[a]	3.0 ± 0.07[a]	2.9 ± 0.05[a]

Abbreviations: Pio, pioglitazone; Rosi, rosiglitazone; SBP, systolic blood pressure.
[a]Diabetic *db/db* versus non-diabetic *db/m* control, $P<0.05$.
[b]Final versus initial, $P<0.05$.

$P<0.05$ (Table 2). There were no differences in tail-cuff systolic blood pressures over the 12-week study. At killing, body weight/tibia length was significantly higher in non-diabetic compared with diabetic mice, $P<0.05$. Kidney weight/tibia length was slightly less in the non-diabetic versus the diabetic $OPN^{+/+}$, $P<0.05$, but remained unchanged in $OPN^{-/-}$mice.

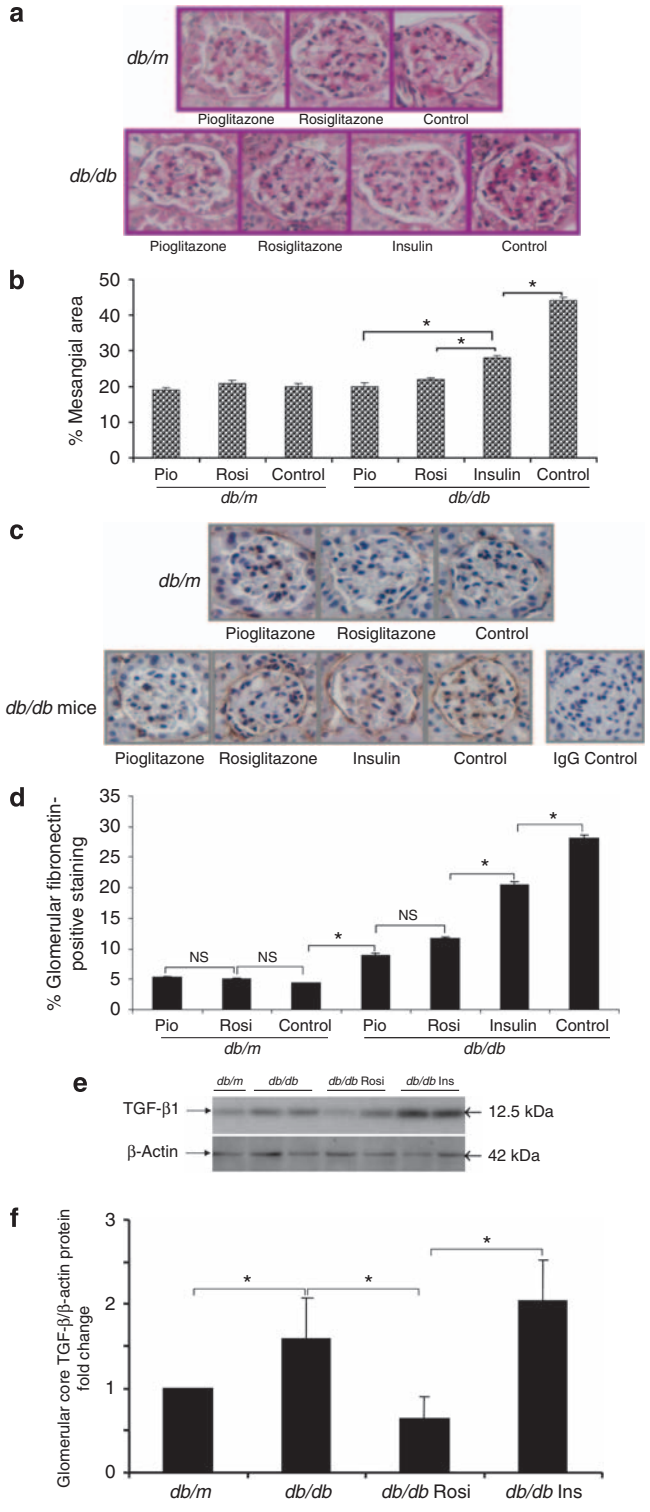

The initial ACR was higher in $OPN^{+/+}$ compared with $OPN^{-/-}$mice, $P<0.05$ (Figure 4a). After 4, 8, and 12 weeks of STZ administration, the diabetic $OPN^{-/-}$ had higher ACR compared with non-diabetic $OPN^{+/+}$ mice. However, ACR in diabetic $OPN^{+/+}$ was substantially higher than in diabetic $OPN^{-/-}$ mice throughout the study. Thus, the lack of OPN attenuated albuminuria after STZ administration, despite similar plasma glucose levels.

To further investigate the effect of OPN on the pathology of DN, kidneys were sectioned for PAS and IHC staining, and glomerular cores were isolated for western blots. STZ-diabetic $OPN^{+/+}$ had greater glomerular % mesangial area (1.9-fold), collagen IV (2.5-fold), TGF-β (1.6-fold), and fibronectin (1.2-fold) expression compared with non-diabetic $OPN^{+/+}$ mice, $P<0.05$ (Figures 4b–i). Collagen, TGF-β, and fibronectin protein levels were not different in STZ-diabetic $OPN^{-/-}$ versus non-diabetic $OPN^{-/-}$ mice. Quantitative RT-PCR of glomerular core collagen IV, fibronectin, and TGF-β expression showed parallel results (data not shown). Thus, the lack of OPN is associated with less albuminuria as well as less glomerular matrix, collagen IV, TGF-β, and fibronectin mRNA and protein, suggesting that OPN may have a pathophysiologic role in glomerular injury in diabetes.

OPN deletion in $Ins2^{akita/+}$ and $Lepr^{db/db}$ mice attenuates albuminuria, glomerular matrix, collagen IV, fibronectin, and TGF-β

To further test the role of OPN in genetic models of types 1 and 2 DN, $OPN^{-/-}$ mice were bred onto $Ins2^{akita/+}$; $Ins2^{+/+}$ and ($Lepr^{db/db}$; $Lepr^{+/+}$ mice) (Figures 5 and 6). Quantitative RT-PCR of glomerular cores confirmed the absence of OPN expression in $OPN^{-/-}$ mice (data not shown). In both groups, initial and final plasma glucose was significantly lower in non-diabetic ($OPN^{+/+}Ins2^{+/+}$; $OPN^{-/-}Ins2^{+/+}$ and $OPN^{+/+}Lepr^{+/+}$; $OPN^{-/-}Lepr^{+/+}$) compared with diabetic ($OPN^{+/+}Ins2^{akita/+}$; $OPN^{-/-}Ins2^{akita/+}$, and $OPN^{+/+}Lepr^{db/db}$; $OPN^{-/-}Lepr^{db/db}$) mice, $P<0.05$. There were no differences in initial or final blood pressures among

Figure 2 | Periodic acid Schiff stain, % mesangial area, fibronectin and TGF-β expression of treated *db/db* mice. After 8 weeks of treatment with pioglitazone (Pio), rosiglitazone (Rosi), insulin or chow-fed Control, *db/db* and *db/m* mice were killed. (**a**) Kidneys were harvested, fixed in 4% paraformaldehyde, and 3 μm sections were stained with Periodic acid Schiff (PAS). (**b**) PAS-positive tissue was quantified as % of total mesangial area measured by optical microscopy image analyses, $^*P<0.05$. (**c**) Kidney sections were used for immunohistochemical staining for fibronectin. Stained Control section shows lack of staining. (**d**) Positive staining for fibronectin in the glomeruli was quantified by optical microscopy. NS: not significant, $^*P<0.001$. (**e**) Protein obtained from isolated glomerular cores was used for western blot analysis of TGF-β expression using autoradiography and (**f**) quantified by densitometry. The figure shows a representative blot (top panel) and bar graph obtained from densitometric analysis of several blots, $^*P<0.05$ (*db/m* control $n=8$, *db/db* control $n=9$, *db/db* Rosi $n=4$, *db/db* Ins $n=4$).

the groups. However, there was a significant increase in body weight and kidney weight/tibia length between $Lepr^{db/db}$ and $Lepr^{+/+}$ mice, $P<0.05$ (Tables 3 and 4).

The protective effect of OPN depletion against albuminuria was demonstrated in genetic type 1 and 2 $OPN^{-/-}$ mice. ACR was 5- to 7.7-fold higher in $OPN^{+/+}Ins2^{akita/+}$ versus $OPN^{+/+}Ins2^{+/+}$ but not different in $OPN^{-/-}Ins2^{akita/+}$ versus $OPN^{-/-}Ins2^{+/+}$ mice at 2, 3, and 4 months, $P<0.05$. Similarly, ACR was ~9-fold higher in $OPN^{+/+}Lepr^{db/db}$ versus $OPN^{+/+}Lepr^{+/+}$ and three- to fourfold higher in $OPN^{-/-}Lepr^{db/db}$ versus $OPN^{-/-}Lepr^{+/+}$ mice, $P<0.05$. OPN deletion attenuated ACR two- to threefold in both genetic $OPN^{-/-}$-diabetic mice, $P<0.05$ (Figures 7a, b).

OPN deletion markedly attenuated the diabetes-induced increases in % mesangial area (~1.3-fold), collagen IV (~1.5-fold), and fibronectin (four to fivefold) in both diabetic models by PAS and IHC, $P<0.05$ (Figures 8a–l; $P<0.001$). Glomerular TGF-β by quantitative RT-PCR showed ~2-fold lower expression in both $OPN^{-/-}$-diabetic models versus diabetic $OPN^{+/+}$ mice, $P<0.01$ and there was no increase in TGF-β expression in diabetic versus non-diabetic $OPN^{-/-}$ mice (Figures 8m, n).

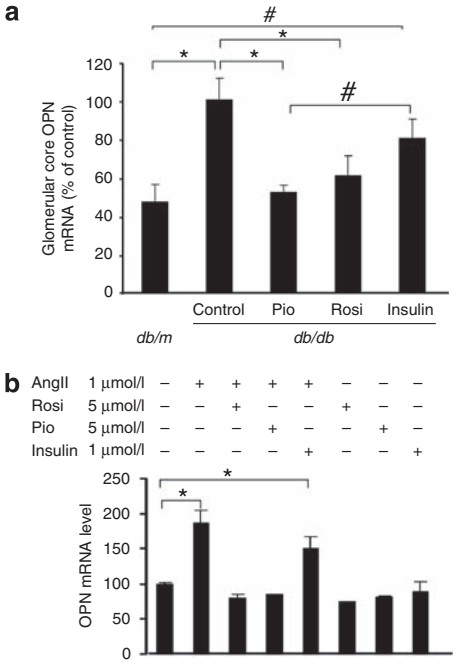

Figure 3 | PPARγ ligands and insulin differentially regulate osteopontin. At the end of the study, mRNA was isolated from glomerular cores of *db/m* and *db/db* mice treated with pioglitazone (Pio), rosiglitazone (Rosi), insulin or control. (**a**) Quantitative RT-PCR analysis of osteopontin (OPN) expression was performed; $^{*}P<0.05$ versus *db/db* control, $^{\#}P<0.05$ versus *db/db* insulin, $n=4$–6. (**b**) Mouse mesangial cells were preincubated with Pio (5 μmol/l) or Rosi (5 μmol/l) followed by treatment with angiotensin II (AngII; 1 μmol/l) or insulin (1 μmol/l); $n=2$–3, $^{*}P<0.05$ versus untreated control cells.

OPN stimulates TGF-β, ERK/MAPK, and JNK signal transduction in mesangial cells

To investigate the cellular effect of OPN, cultured mesangial cells were incubated with recombinant mouse OPN (rmOPN) for up to 24 h. There was a dose-dependent increase in TGF-β expression with OPN up to 10 nM (Figure 9a, b). At 10 nM, there was a time-dependent upregulation of OPN by TGF-β (Figure 9c, d), which peaked at 12 h. In contrast, pretreatment of mesangial cells grown in high glucose (30 mM) with antibody against OPN resulted in a dose-dependent inhibition of TGF-β expression (Figure 9e, f). These data suggested that OPN enhances TGF-β expression, and that OPN may promote glomerular matrix accumulation by upregulation of TGF-β.

Several studies have shown that mitogen-activated protein kinase (MAPK) signaling pathways are activated in mesangial cells in the diabetic milieu. To understand the potential mechanisms by which OPN may regulate extracellular matrix expression and thus identify a potential link to promote albuminuria in the glomerulus, mesangial cells were preincubated with inhibitors of ERK/MAPK (PD98059) and JNK/MAPK (SP600125) for 30 min followed by incubation with rmOPN for 30 and 45 min, respectively. Phosphorylated ERK and phosphorylated JNK were upregulated two- to threefold by rmOPN, $P<0.05$. However, only ERK and not JNK expression was significantly inhibited after preincubation with the inhibitor (Figures 10a–d). As c-Jun is phosphorylated by JNK at serine 63,[13] we looked at the expression of c-Jun to determine whether the ability of activated JNK to phosphorylate c-Jun is altered. We showed a

Table 2 | Physiological characteristics of $OPN^{+/+}$ and $OPN^{-/-}$ mice

	$OPN^{+/+}$		$OPN^{-/-}$	
	Control	Diabetic	Control	Diabetic
Number of mice	10	13	8	10
Initial plasma glucose (mg/dl)	63 ± 4	68 ± 4	73 ± 7	68 ± 3
Final plasma glucose (mg/dl)	93 ± 5[a]	601 ± 24[a]	102 ± 8[a]	462 ± 56[a]
Initial SBP (mm Hg)	93 ± 5	100 ± 5	94 ± 6	88 ± 4
Final SBP (mm Hg)	101 ± 3	97 ± 4	101 ± 5	105 ± 2
Body weight/tibia length (g/mm)	1.9 ± 0.1[b]	1.4 ± 0.1	1.9 ± 0.0[b]	1.6 ± 0.1
Kidney weight/tibia length (g/mm)	0.01 ± 0.0[b]	0.02 ± 0.0	0.01 ± 0.0	0.01 ± 0.0

Abbreviation: SBP, systolic blood pressure.
[a]Final versus initial, $P<0.05$.
[b]Control versus diabetic, $P<0.05$.

significant downregulation of phosphorylated c-Jun, $P<0.05$ (Figures 10e, f) suggesting that OPN impacts the downstream activity of JNK. These results are in keeping with previous investigation in osteoblastic cells, in which activation of ERK/MAPK and c-Jun occurred during cellular adhesion to OPN-coated plates.[14]

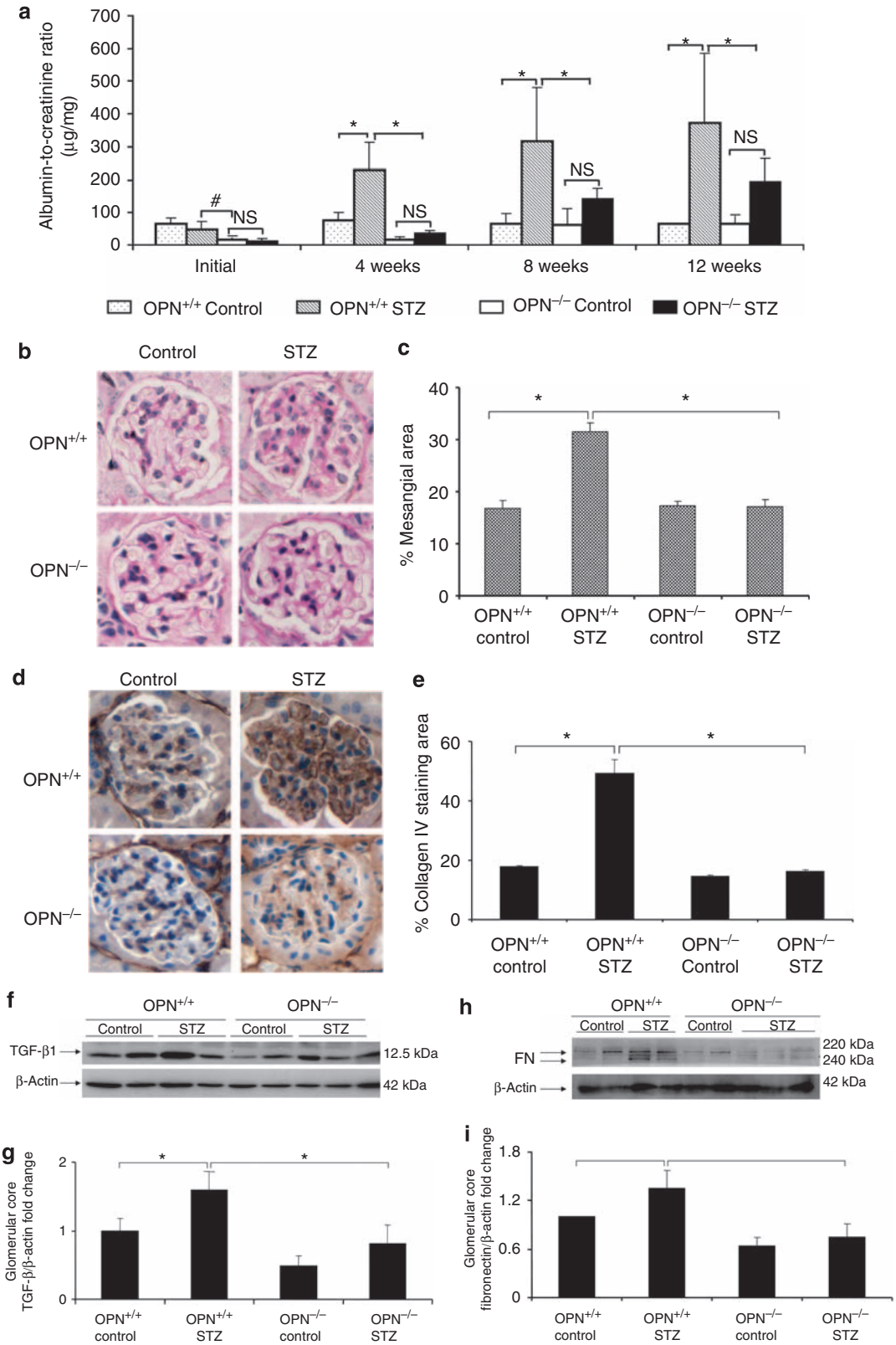

DISCUSSION

In this investigation, two PPARγ ligands, rosiglitazone and pioglitazone, attenuated albuminuria in the *db/db* C57BLKS/J^{lepr} mouse which, to date, is one of the better known models of human type 2 DN.[12,15] Although insulin administration to *db/db* mice lowered plasma glucose to the levels comparable to TZDs, it did not attenuate albuminuria to the same extent as PPARγ activation. In previous studies, TZDs decreased albuminuria in humans and *db/db* mice better than other oral antihyperglycemic agents[16–18] and are effective in STZ-treated mice without changes in plasma glucose.[3] Our and other observations that PPARγ is expressed in mesangial cells help to explain these findings, although the mechanisms for the TZD effect has been obscure.[3] *In vitro*, PPARγ activation impaired mesangial cell growth; TGF-β, plasminogen-activator inhibitor-1 and vascular endothelial growth factor production; and TGF-β activity.[3,19,20] We found that TZD or insulin administration both decreased glomerular OPN expression in *db/db* mice across all treatment groups, but OPN was reduced to a greater extent by the TZDs, paralleling their effects on albuminuria. The decrease in glomerular OPN *in vivo* can be attributed, at least in part, to glucose lowering, as OPN expression is increased by hyperglycemia.[21,22] However, this study suggests that TZDs suppress OPN expression beyond glucose lowering. In cultured mesangial cells, TZDs suppressed AngII-induced OPN expression, whereas insulin had no effect. Thus, TZDs have direct actions to inhibit mesangial OPN production, whereas the insulin effect *in vivo* is likely mediated through glucose lowering.

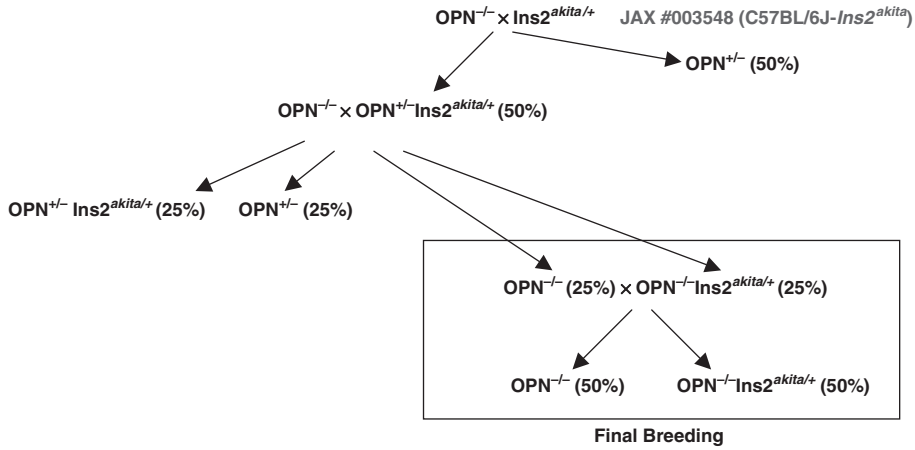

Figure 5 | Breeding protocol for OPN$^{-/-}$ Ins2$^{akita/+}$.

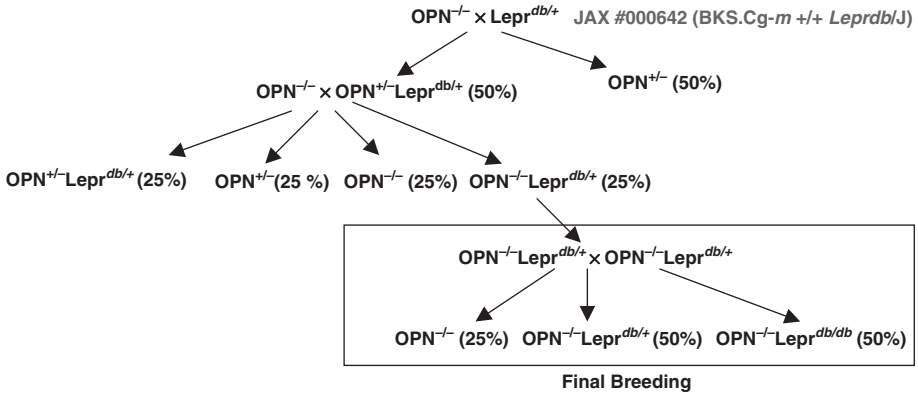

Figure 6 | Breeding protocol for OPN$^{-/-}$ Lepr$^{db/db}$.

Figure 4 | STZ-diabetic OPN knockout mice have significantly reduced albumin-to-creatinine ratio (ACR), glomerular extracellular matrix protein and TGF-β expression. Osteopontin wild-type (OPN$^{+/+}$) and knockout (OPN$^{-/-}$) mice on a 129 × Black Swiss background were made diabetic with streptozotocin (STZ) and assessed for 12 weeks. (**a**) Mice were placed in metabolic cages for 24 h urine collection to obtain ACR (mean ± s.d.); *$P<0.001$, $^{\#}P<0.01$, NS: not significant. (**b–e**) Kidney sections from treated and untreated mice were used for PAS and IHC staining for matrix accumulation, collagen IV and positive staining was quantified by optical microscopy image analyses, *$P<0.05$. (**f–i**) Protein from glomerular cores of streptozotocin (STZ)-induced diabetic and non-diabetic osteopontin wild-type control (OPN$^{+/+}$) and knockout (OPN$^{-/-}$) mice was used in western blots for TGF-β and fibronectin (FN) and standardized to β-actin. Representative western blots (top panels) of TGF-β and FN expression and densitometric analyses (bottom panels) are shown; *$P<0.05$, $n=4$–8. ACR, albumin-to-creatinine ratio; IHC, immunohistochemistry.

Table 3 | Physiological features of diabetic Ins2$^{akita/+}$ and non-diabetic Ins2$^{+/+}$ mice

	OPN$^{+/+}$		OPN$^{-/-}$	
	Ins2$^{+/+}$ Non-diabetic	Ins2$^{akita/+}$ Diabetic	Ins2$^{+/+}$ Non-diabetic	Ins2$^{akita/+}$ Diabetic
Number of mice	10	7	7	8
Initial plasma glucose (mg/dl)	95 ± 3	480 ± 34[a]	73 ± 12	453 ± 40[a]
Final plasma glucose (mg/dl)	117 ± 3.5	465 ± 34[a]	114 ± 10	468 ± 41[a]
Initial SBP (mm Hg)	100 ± 5	94 ± 6	92 ± 3	104 ± 3
Final SBP (mm Hg)	97 ± 4	108 ± 4	96 ± 5	95 ± 5
Body weight/tibia length (g/mm)	1.8 ± 0.06	1.24 ± 0.04	2.02 ± 0.07	1.34 ± 0.03
Kidney weight/tibia length (g/mm)	0.012 ± 0.000	0.014 ± 0.001	0.012 ± 0.000	0.0129 ± 0.000

Abbreviation: SBP, systolic blood pressure.
Initial: age 2 months.
Final: age 4 months.
[a]$P < 0.05$, diabetic versus control mice.

Table 4 | Physiological features of OPN$^{-/-}$Lepr and OPN$^{+/+}$Lepr non-diabetic and diabetic mice

	OPN$^{+/+}$		OPN$^{-/-}$	
	Lepr$^{+/+}$ Non-diabetic	Lepr$^{db/db}$ Diabetic	Lepr$^{+/+}$ Non-diabetic	Lepr$^{db/db}$ Diabetic
Number of mice	9	7	9	15
Initial plasma glucose (mg/dl)	97 ± 7	417 ± 50[a]	85 ± 5	497 ± 35[a]
Final plasma glucose (mg/dl)	116 ± 4	555 ± 29[a,b]	86 ± 9[c]	499 ± 22[a]
Initial SBP (mm Hg)	106 ± 4	100 ± 5	107 ± 4	109 ± 4
Final SBP (mmHg)	105 ± 4	101 ± 4	115 ± ± 4	109 ± 4
Body weight/tibia length (g/mm)	1.70 ± 0.06	2.80 ± 0.18[a]	1.78 ± 0.09	2.60 ± 0.17[a]
Kidney weight/tibia length (g/mm)	0.012 ± 0.001	0.015 ± 0.001[a]	0.011 ± 0.001	0.015 ± 0.001[a]

Abbreviation: SBP, systolic blood pressure.
Initial: age 2 months.
Final: age 4 months.
[a]$P < 0.05$, diabetic versus non-diabetic.
[b]$P < 0.05$, final versus initial.
[c]$P < 0.05$, OPN$^{-/-}$ versus OPN$^{+/+}$.

To define the role of OPN in albuminuria, we induced STZ diabetes in OPN-null mice, which were on a mixed background. As STZ has been suggested to cause renal damage beyond its diabetogenic effect, we studied OPN effects in the Ins2$^{akita/+}$ type 1 diabetic mouse, which has a severe insulin deficiency due to a β-cell insulin processing defect with subsequent renal damage (http://www.amdcc.org). STZ-diabetic OPN$^{-/-}$ mice developed albuminuria that was only 20–50% of diabetic OPN$^{+/+}$, which was associated with decreased glomerular collagen, fibronectin, and TGF-β, suggesting decreased renal profibrotic changes. Similarly, loss of OPN in the Ins2$^{akita/+}$ resulted in ACRs that were 30–50% of diabetic controls and attenuated the diabetes-induced increase in glomerular TGF-β and extracellular matrix proteins. Deletion of OPN in the genetic Lepr$^{db/db}$ type 2 diabetic mouse also caused a 30% reduction in albuminuria and was similarly associated with decreased glomerular collagen, fibronectin, and TGF-β expression. Thus, in three strains of diabetic mice, loss of OPN resulted in substantial reduction of albuminuria and mesangial fibrosis, demonstrating a critical role of OPN in DN. It is important to note here that as mixed backgrounds were used in these studies, genetic differences in the mice cannot be fully excluded as explanations for some of the effects observed. However, the *in vitro* data appear to support the *in vivo* observations. Addition of rmOPN to mesangial cells resulted in a dose- and time-dependent stimulation of TGF-β, whereas OPN antibodies inhibited the hyperglycemia-induced rise in OPN. Taken together, these results suggest that OPN is a key profibrotic factor contributing to the development of glomerulosclerosis and albuminuria in diabetes.

OPN was first isolated from bone[23–25] and later identified in other tissues and cells, including the vasculature, heart, as well as renal tubules and glomerular epithelial cells, and several body fluids suggesting it is secreted by cells.[26,27] Its diverse functions regulate tissue calcification and promote inflammation, tissue remodeling, fibrosis, and angiogenesis.[28] Many of these effects are mediated by the binding of OPN to cell surface integrin receptors, such as αvβ1, αvβ3, αvβ5, which activate intracellular signaling pathways.[29] In the kidney, OPN appears to be protective against accumulation of calcium oxalate stones.[30–32] However, it has been associated with renal diseases characterized by tubulointerstitial fibrosis and proteinuria, as well as DN.[33–35]

The finding that OPN is differentially regulated by PPARγ ligands is of interest. The beneficial renal effect of PPARγ agonists in type 2 diabetes is likely mediated in part through their antiglycemic effect.[18] Treatment with rosiglitazone can improve glomerular filtration rate, filtration fraction, and endothelial function, possibly by increased nitric oxide bioavailability[36] TZDs also inhibit podocyte apoptosis,[37] which contributes to albuminuria and progressive proteinuria.[38–40] Thus, several mechanisms potentially contribute to the

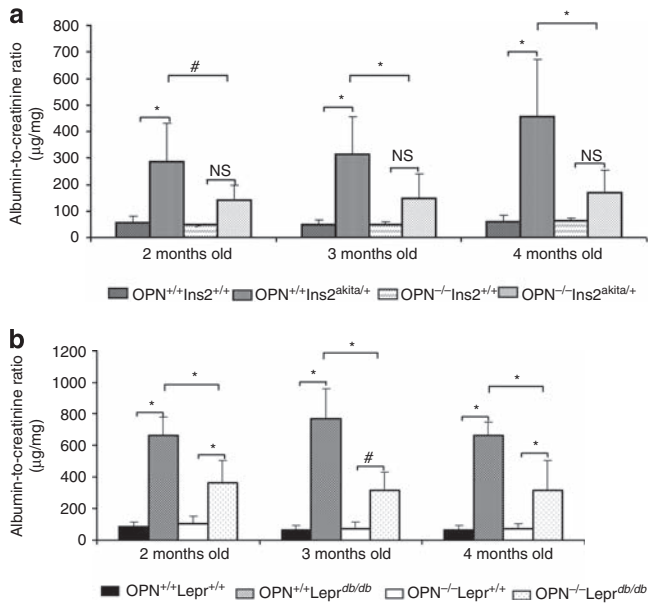

Figure 7 | OPN deletion protects against albuminuria in type 1 Ins2$^{akita/+}$ and type 2 *db/db* diabetic mice. OPN$^{-/-}$ mice were bred against Ins2$^{+/+}$; Ins2$^{akita/+}$ and *db/m* (Lepr$^{db/+}$) and *db/db* (Lepr$^{db/db}$) mice to generate genetic models of type 1 and 2 diabetes OPN-null mice and their corresponding littermates. Animals were placed in metabolic cages after 2, 3, and 4 months for urine collection. (**a** and **b**) In both models, albumin-to-creatinine ratio (mean ± s.d.) was significantly higher in diabetic versus non-diabetic OPN$^{+/+}$ mice, $^{*}P<0.001$, $^{\#}P<0.01$, NS, not significant.

protective effects of TZDs in DN in addition to their action to suppress glomerular OPN.

PPARγ ligands attenuate inflammatory gene expression by inhibition of AP-1 and nuclear factor-κB sites.[41] Recently, Pascual *et al.*[42] identified a novel mechanism of active gene repression: PPARγ ligands prevented removal of the corepressor NCOR from an inflammatory response gene promotor by preventing the recruitment of the proteosome machinery, which normally degrades NCOR by ubiquitylation. Active corepresssion did not involve a PPARγ response element. Although, the OPN promoter does not have a PPARγ response element or nuclear factor-κB site, it does have multiple AP-1 sites.[43–45] Troglitazone was reported to suppress OPN in THP-1 macrophages at a non-AP-1 site at −89 to −95 in the OPN promoter.[11] The importance of this site has not been confirmed. Further studies are necessary to detail the mechanisms by which PPARγ ligands suppress OPN, which can ultimately attenuate fibrosis and inflammation.

In this study, OPN stimulated TGF-β *in vitro*, while the effect of OPN deletion *in vivo* decreased glomerular TGF-β. Thus, in addition to promoting tissue macrophage recruitment, cell growth and adhesion, OPN may enhance fibrogenesis by direct TGF-β stimulation and subsequent extracellular matrix production.[46] Furthermore, rmOPN activated ERK/MAPK and JNK (through c-Jun activation) signaling pathways, which are known to stimulate TGF-β production in mesangial cells.[8,47] OPN antibodies inhibited glucose-induced TGF-β expression, suggesting that OPN mediates some of the adverse effects of glucose. In a previous study, hyperglycemia and hypoxia additively stimulated OPN mRNA and protein expression, leading to increased collagen IV and cell proliferation[8,22] that were blocked by neutralizing antibody to either OPN or β3-integrin receptor, pointing to a profibrotic role for OPN. Taken together, these data suggest that modalities that decrease OPN or block β_3-integrin may be useful therapeutic targets in DN.

In a mouse model of obstructive uropathy, Ophascharoensuk *et al.*[48] demonstrated decreased renal interstitial fibrosis in OPN$^{-/-}$ mice, and decreased macrophage accumulation. Indeed, inflammation contributes to tissue fibrosis, and macrophages from OPN$^{-/-}$ animals demonstrate increased apoptosis, decreased migration and altered inflammatory behavior compared with macrophages of controls.[49] Recently, the role of inflammation, and particularly macrophage chemoattractant protein-1 (MCP-1) was examined in the development of DN in both STZ-diabetic and diabetic *db/db* mice.[50–52] Lack of MCP-1 was associated with a marked reduction in glomerular and interstitial macrophage accumulation, albuminuria, and renal fibrosis.[50,51] We previously demonstrated in the heart that (1) OPN is upregulated in cardiac hypertrophy along with brain natriuretic peptide, (2) rmOPN promotes cardiac fibroblast adhesion to a variety of extracellular matrices, and (3) OPN$^{-/-}$ mice have attenuated AngII-induced cardiac fibrosis, suggesting that OPN mediates interstitial fibrosis in the heart similar to its impact in the kidney.[53] However, in the heart, AngII promotes fibrosis, in large part, by promoting a substantial interstitial and perivascular inflammatory response,[54,55] that is not as profound as the inflammatory response in DN.[56,57] Thus, direct OPN actions in mesangial cells to stimulate TGF-β and matrix deposition appear to be important mechanisms by which OPN contributes to DN.

In summary, mounting evidence supports the role of OPN in mediating the fibrotic changes associated with glomerulosclerosis and interstitial fibrosis, hallmarks of DN. OPN may be a novel therapeutic target in profibrotic diseases. RAAS activation is associated with enhanced tissue OPN expression, and RAAS blockade downregulates OPN expression[58,59] and thus may have additive or synergistic actions with PPARγ activation in decreasing renal OPN and proteinuria. The present observations support the development of clinical studies examining the potential protective effects of PPARγ ligands in both type 1 and 2 DN.

MATERIALS AND METHODS

Animals

Genetic models of type 1 and 2 diabetic OPN$^{-/-}$ mice were bred into JAX#003548 C57BL6-*Ins2^{akita}*/J and JAX#000642 BKS.Cg-*Dock7$^{m+/+}$ Lepr^{db}*/J (purchased from Jackson Labs, Bar Harbor, ME, USA), respectively. The presence or absence of the Ins2^{akita} mutant within each colony were littermates, Lepr^{db} heterozygotes

were bred together to produce lepr$^{db/db}$ and lepr$^{+/+}$ littermates within OPN-expressing and OPN-deficient mice, which were produced after three generations (Figures 5 and 6) and the colony mates were controls. Diabetic *db/db* mice were fed rosiglitazone (367 mg/kg/day), pioglitazone (300 mg/kg/day) or administered insulin (1–4 U/kg) for comparable plasma glucose (~300 mg/dl). Breeding pairs of OPN$^{-/-}$ (129 × Black Swiss background) with the mutated secreted phosphoprotein 1 (*spp-1*) gene for OPN were a gift of R. Johnson and C.M. Giachelli (University of Florida, Gainesville, FL, USA) with permission from L. Liaw (Maine Medical Center Research Institute, South Portland, ME, USA).[49,60] OPN$^{+/+}$ and OPN$^{-/-}$ mice were made diabetic by intraperitoneal STZ (2.5 mg/kg). Mice were fed normal chow (Harlan 8604) *ad lib* at 12 h light–dark cycles. Procedures were approved by the UCLA Animal Research Committee and complied with appropriate federal, state, local and institutional regulations.

Physiological measurement

Fasting plasma glucose from retro-orbital blood for glucose oxidase reaction (Beckman Glucose Analyzer 2, Beckman Instruments,

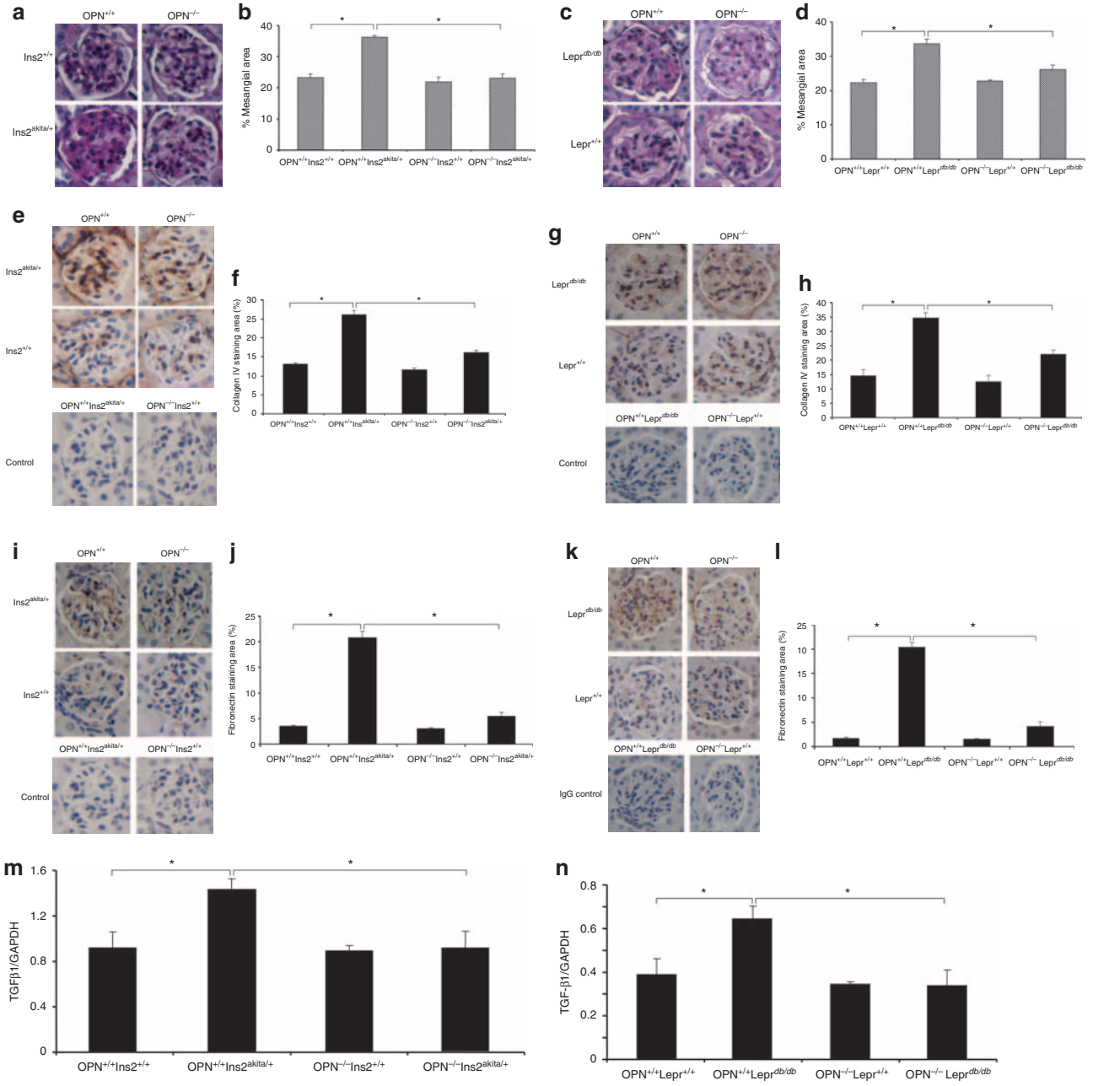

Figure 8 | OPN deletion protects against renal changes in type 1 Ins2$^{akita/+}$ and type 2 *db/db* diabetic mice. At the end of the study, kidney sections were used for analysis by PAS staining (**a–d**) and IHC of collagen IV and fibronectin and quantified. (**e–l**) The figures show quantification of % mesangial area from 25 non-overlapping randomly selected fields of each glomeruli/animal section and glomerular staining for collagen IV and fibronectin (15 fields). Signals were measured by computerized image analysis, *$P < 0.001$, $n = 4$–6. (**m,n**) RNA was isolated from glomerular cores and analyzed by quantitative RT-PCR for TGF-β expression; *$P < 0.01$, $n = 4$–6.

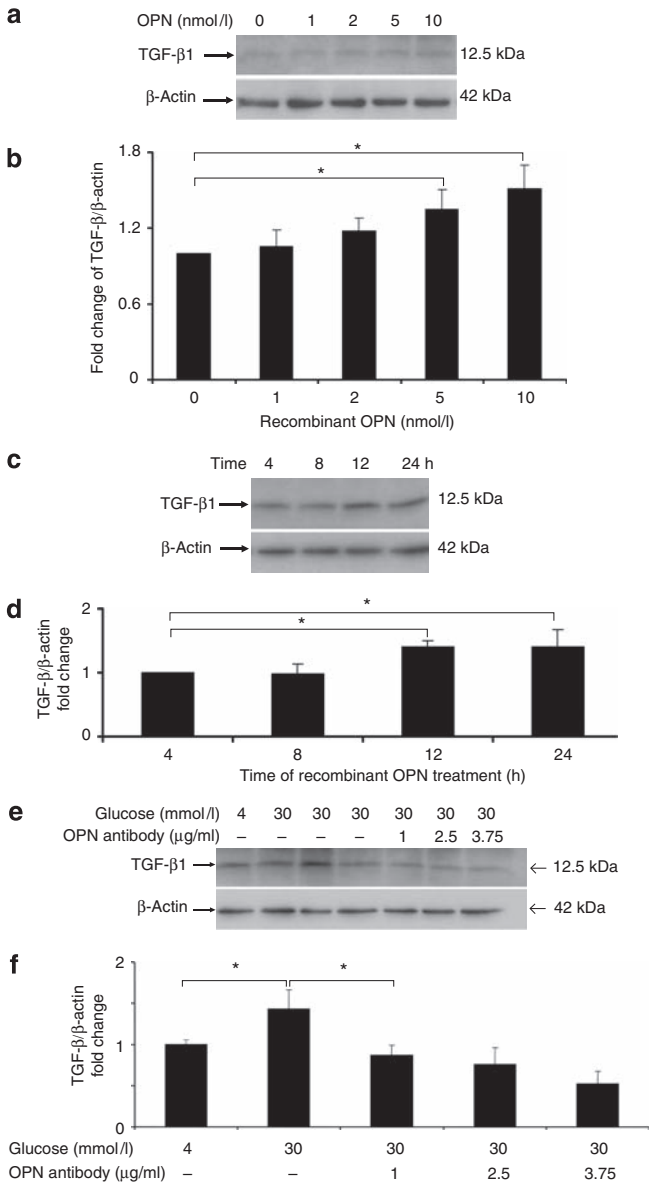

Figure 9 | OPN induces TGF-β in a dose-dependent and time-dependent manner. Stable mouse mesangial cells (MES 13) were used for *in vitro* experiments for mRNA and protein expression (representative western blots shown). (**a** and **b**) Mesangial cells were treated with increasing concentrations of rmOPN (0–10 nmol/l) for 24 h; $n = 4$, $^*P < 0.05$. (**c** and **d**) Mesangial cells were treated with rmOPN (10 nmol/l) for up to 24 h, $n = 4$, $^*P < 0.05$ versus 4 h treatment. (**e** and **f**) Mesangial cells were grown in glucose (4 or 30 mmol/l) or pretreated for 2 h with increasing concentrations of OPN antibody, $n = 4$. After 48 h, cells were lysed and the protein used in western blot analysis. The figure shows a representative western blot and quantification of TGF-β1/β-actin signal, $^*P < 0.05$ versus cells in glucose 4 mmol/l. rmOPN, recombinant mouse osteopontin.

Fullerton, CA, USA) on ⩾3 repeated fasted blood samples were measured and averaged. Weekly blood pressures were obtained from trained, prewarmed mice by computerized, non-invasive tail-cuff system (BP 2000 Blood Pressure Analysis System, Visitech System, Apex, NC, USA). Animals were placed in humidified metabolic cages for 24 h urine collection. Urinary creatinine and albumin measurements were performed by Creatinine Companion and Albumin M assay (Exocel, Philadelphia, PA, USA), respectively. Kidneys were dissected, weighed, and tibia lengths were measured to reduce effects of changes in body weight.

Periodic acid Schiff staining

At the end of treatment (age 16 weeks), kidney tissues were immersion-fixed in 4% paraformaldehyde/phosphate-buffered saline, and embedded in paraffin. Sections (3 μm) were stained with PAS for matrix (http://www.amdcc.org). Twenty-five glomeruli from ⩾5 animals per group were digitally quantified and reported as % mesangial area.

Immunohistochemistry staining

Fibronectin and collagen IV expression in kidney sections was detected by IHC, by avidin–biotin immunoperoxidase (ZYMED detection system; Carlsbad, CA, USA). Paraffin-embedded 4 μm sections were deparaffinized with xylene, rehydrated in descending series of ethanol and boiled in 10 mmol/l citrate buffer. Endogenous peroxidase was applied in 10% hydrogen peroxide in phosphate-buffered saline × 10 min and sections were blocked with avidin/biotin blocking reagent. Primary antibodies against mouse fibronectin and collagen IV (1:200; Lab Vision, Fermont, CA, USA) or phosphate-buffered saline (negative control) were incubated overnight at 4°C. The sections were washed in phosphate-buffered saline, incubated with secondary antibodies, washed and incubated × 30 min with Vectastain ABC reagent (Burlingame, CA, USA). Bound antibodies were detected using substrate-chromagen mixture for a brown color. The sections were stained with hematoxylin solution, dehydrated, and evaluated by light microscopy. Fibronectin and collagen IV staining was quantified by scanning 15 non-overlapping randomly selected fields/kidney sections at × 200 magnification (with exclusion of blood vessel areas). The percentage of the immunohistochemical signal was measured by computerized image analysis system (Image Pro-Plus, Media Cybernetics, Silver Spring, MD, USA).

Western blot analysis

Western blot analysis was performed using standard procedures. Mouse glomerular cores were isolated by the sieving method.[61] Briefly, mouse kidney cortex was excised and passed through sieves of 60, 100, and 200 mesh for glomerular tufts of glomerular cells. Glomerular core protein (40–100 μg) was separated by sodium dodecyl sulfate-polyacrylamide gel electrophoresis. Membranes were probed with primary antibody to fibronectin (mouse anti-fibronectin antibody, 1:100; Lab Vision, Fremont, CA, USA), TGF-β (rat anti-TGF-β antibody; 1:100 dilution; BD Pharmingen, San Diego, CA, USA), phosphorylated and total ERK/MAPK, JNK and c-Jun. Membranes were incubated with secondary antibody (anti-mouse IgG, 1:2500, Cell Signaling Technology, Danvers, MA, USA; or anti-rat IgG, 1:2000, Amersham Biosciences, Piscataway, NJ, USA). The signals were scanned and quantified by ArcSoft photostudio v.5 software (Fremont, CA, USA). Following enhanced chemiluminescence detection, the membranes were stripped and proteins rehybridized with anti-β-actin antibody (1:3500, Gene Tex, San Antonio, TX, USA). Protein levels expressed as protein/β-actin ratio minimized loading differences.

Quantitative RT-PCR

Total RNA from glomerular cores or cell lysate isolated by RNeasy (Qiagen, Valencia, CA, USA) was treated with DNase (Promega,

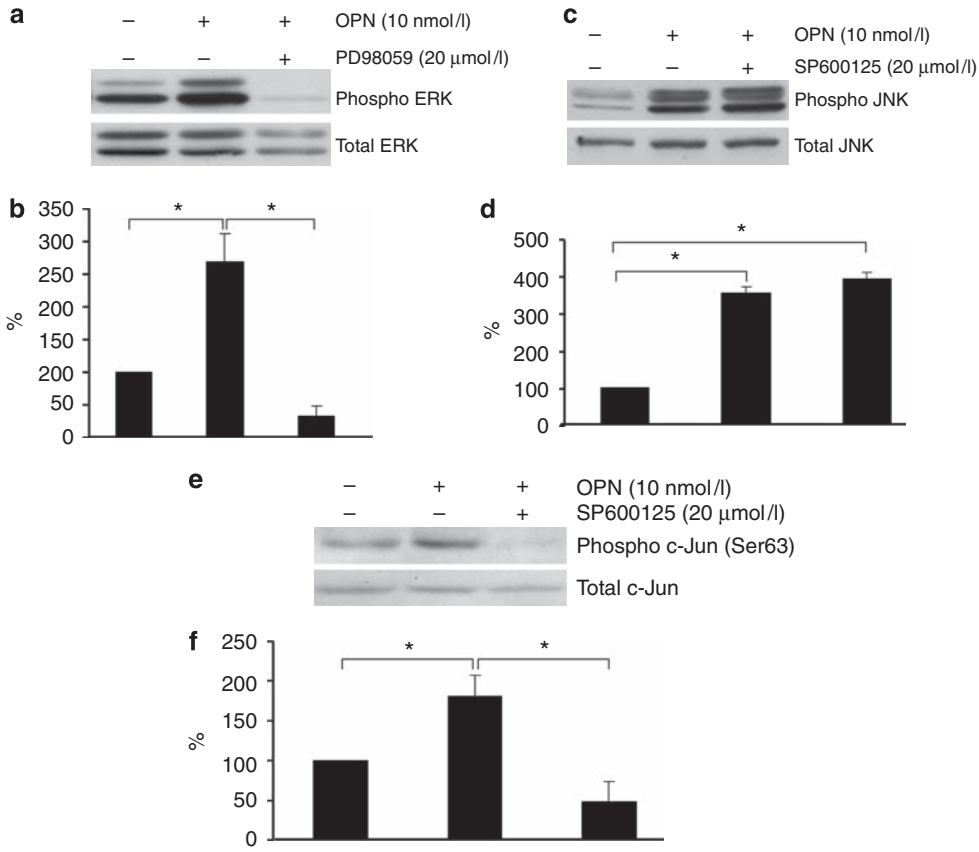

Figure 10 | Recombinant OPN stimulates ERK/MAPK and JNK signal transduction. Stable mouse mesangial cells (MES 13) were grown in culture and preincubated with inhibitors of ERK/MAPK (PD98059; 20 μmol/l) and JNK/MAPK (SP600125; 20 μmol/l) for 30 min followed by treatment with recombinant OPN (10 nmol/l) for 30 and 45 min, respectively. Representative western blots and densitometric quantification for (**a** and **b**) phosphorylated ERK and total ERK and (**c** and **d**) phosphorylated JNK and total JNK. (**e** and **f**) Phosphorylated c-Jun and total c-Jun; $n = 3$–4 separate experiments, *$P < 0.05$ OPN versus OPN + inhibitor.

Madison, WI, USA). Reverse transcription was performed using TaqMan Reverse Transcription Reagents (Applied Biosystems, Foster City, CA, USA). The synthesized cDNA was quantified by quantitative RT-PCR using ABI Prism 7700 Sequence Detection System (Applied Biosystems) as follows: 50°C × 2 min, 95°C × 10 min, 95°C × 1 s and 60°C × 1 min for 40 cycles using primers (200 nmol/l) and probes (100 nmol/l). PCR amplifications of 20× reagent of proprietary reverse and forward primers and probes for OPN (25 μl; ABI, Mm00437304_m1, Assay-on-Demand Gene Expression Products, Applied Biosystems) were performed in triplicates. Gene expression compared with GAPDH was measured simultaneously, $n = 4$ separate experiments.

Mouse mesangial (MES-13) cell culture

Stable mouse mesangial cells (American Type Culture Collection, Manassas, VA, USA) were grown to 90% confluence, serum-starved (0.05% fetal bovine serum) × 18–24 h and treated with insulin (1 μmol/l), angiotensin II (AngII; 1 μmol/l), pioglitazone (5 μmol/l) or rosiglitazone (5 μmol/l) for 24–48 h or rmOPN (0–10 nmol/l; R&D Systems, Minneapolis, MN, USA) for up to 24 h. Cells were lysed and RNA and protein were isolated for OPN expression by quantitative RT-PCR and western blot.

Statistical analysis

Data are expressed as the mean ± s.e. of the mean or s.d. where stated. We assessed differences between control and treated groups using Student's *t*-test and between multiple groups using analysis of varincce with Tukey's multiple-comparisons post-test where $P < 0.05$. Data sets were tested for normality and statistical significance ($P < 0.05$) using InStat Statistical software (San Diego, CA, USA).

DISCLOSURE

All the authors declared no competing interests.

ACKNOWLEDGMENTS

This work was supported by a grant from the National Institutes of Health, (DK-30254-16 to WAH), GlaxoSmith Kline and the Marion and Bob Wilson Foundation. We thank Stacy Robinson for her valuable assistance.

REFERENCES

1. Imano E, Kanda T, Nakatani Y *et al.* Effect of troglitazone on microalbuminuria in patients with incipient diabetic nephropathy. *Diabetes Care* 1998; **21**: 2135–2139.
2. Isshiki K, Haneda M, Koya D *et al.* Thiazolidinedione compounds ameliorate glomerular dysfunction independent of their insulin-sensitizing action in diabetic rats. *Diabetes* 2000; **49**: 1022–1032.
3. Nicholas SB, Kawano Y, Wakino S *et al.* Expression and function of peroxisome proliferator-activated receptor-gamma in mesangial cells. *Hypertension* 2001; **37**: 722–727.
4. Tanimoto M, Fan Q, Gohda T *et al.* Effect of pioglitazone on the early stage of type 2 diabetic nephropathy in KK/Ta mice. *Metabolism* 2004; **53**: 1473–1479.
5. Endlich N, Sunohara M, Nietfeld W *et al.* Analysis of differential gene expression in stretched podocytes: osteopontin enhances

adaptation of podocytes to mechanical stress. *FASEB J* 2002; **16**: 1850–1852.
6. Giachelli CM. Vascular calcification: *in vitro* evidence for the role of inorganic phosphate. *J Am Soc Nephrol* 2003; **14**: S300–S304.
7. Giachelli CM, Liaw L, Murry CE *et al.* Osteopontin expression in cardiovascular diseases. *Ann NY Acad Sci* 1995; **760**: 109–126.
8. Sodhi CP, Batlle D, Sahai A. Osteopontin mediates hypoxia-induced proliferation of cultured mesangial cells: role of PKC and p38 MAPK. *Kidney Int* 2000; **58**: 691–700.
9. Susztak K, Bottinger E, Novetsky A *et al.* Molecular profiling of diabetic mouse kidney reveals novel genes linked to glomerular disease. *Diabetes* 2004; **53**: 784–794.
10. Oyama Y, Akuzawa N, Nagai R *et al.* PPARgamma ligand inhibits osteopontin gene expression through interference with binding of nuclear factors to A/T-rich sequence in THP-1 cells. *Circ Res* 2002; **90**: 348–355.
11. Oyama Y, Kurabayashi M, Akuzawa N *et al.* Troglitazone, a PPARgamma ligand, inhibits osteopontin gene expression in human monocytes/macrophage THP-1 cells. *J Atheroscler Thromb* 2000; **7**: 77–82.
12. Breyer MD, Bottinger E, Brosius III FC *et al.* Mouse models of diabetic nephropathy. *J Am Soc Nephrol* 2005; **16**: 27–45.
13. Johnson GL, Nakamura K. The c-jun kinase/stress-activated pathway: regulation, function and role in human disease. *Biochim Biophys Acta* 2007; **1773**: 1341–1348.
14. Lee YJ, Park SJ, Lee WK *et al.* MG63 osteoblastic cell adhesion to the hydrophobic surface precoated with recombinant osteopontin fragments. *Biomaterials* 2003; **24**: 1059–1066.
15. Breyer MD, Bottinger E, Brosius FC *et al.* Diabetic nephropathy: of mice and men. *Adv Chronic Kidney Dis* 2005; **12**: 128–145.
16. Bakris GL, Ruilope LM, McMorn SO *et al.* Rosiglitazone reduces microalbuminuria and blood pressure independently of glycemia in type 2 diabetes patients with microalbuminuria. *J Hypertens* 2006; **24**: 2047–2055.
17. Hsueh WA, Nicholas SB. Peroxisome proliferator-activated receptor-gamma in the renal mesangium. *Curr Opin Nephrol Hypertens* 2002; **11**: 191–195.
18. Sarafidis PA, Lasaridis AN, Nilsson PM *et al.* The effect of rosiglitazone on urine albumin excretion in patients with type 2 diabetes mellitus and hypertension. *Am J Hypertens* 2005; **18**: 227–234.
19. Onozaki A, Midorikawa S, Sanada H *et al.* Rapid change of glucose concentration promotes mesangial cell proliferation via VEGF: inhibitory effects of thiazolidinedione. *Biochem Biophys Res Commun* 2004; **317**: 24–29.
20. Weigert C, Brodbeck K, Bierhaus A *et al.* c-Fos-driven transcriptional activation of transforming growth factor beta-1: inhibition of high glucose-induced promoter activity by thiazolidinediones. *Biochem Biophys Res Commun* 2003; **304**: 301–307.
21. Mori S, Takemoto M, Yokote K *et al.* Hyperglycemia-induced alteration of vascular smooth muscle phenotype. *J Diabetes Complications* 2002; **16**: 65–68.
22. Sodhi CP, Phadke SA, Batlle D *et al.* Hypoxia and high glucose cause exaggerated mesangial cell growth and collagen synthesis: role of osteopontin. *Am J Physiol Renal Physiol* 2001; **280**: F667–F674.
23. Hunter GK, Hauschka PV, Poole AR *et al.* Nucleation and inhibition of hydroxyapatite formation by mineralized tissue proteins. *Biochem J* 1996; **317**(Part 1): 59–64.
24. Hunter GK, Kyle CL, Goldberg HA. Modulation of crystal formation by bone phosphoproteins: structural specificity of the osteopontin-mediated inhibition of hydroxyapatite formation. *Biochem J* 1994; **300**(Part 3): 723–728.
25. Prince CW, Oosawa T, Butler WT *et al.* Isolation, characterization, and biosynthesis of a phosphorylated glycoprotein from rat bone. *J Biol Chem* 1987; **262**: 2900–2907.
26. Higashibata Y, Sakuma T, Kawahata H *et al.* Identification of promoter regions involved in cell- and developmental stage-specific osteopontin expression in bone, kidney, placenta, and mammary gland: an analysis of transgenic mice. *J Bone Miner Res* 2004; **19**: 78–88.
27. Weber GF. The metastasis gene osteopontin: a candidate target for cancer therapy. *Biochim Biophys Acta* 2001; **1552**: 61–85.
28. Canfield AE, Farrington C, Dziobon MD *et al.* The involvement of matrix glycoproteins in vascular calcification and fibrosis: an immunohistochemical study. *J Pathol* 2002; **196**: 228–234.
29. Yokosaki Y, Tanaka K, Higashikawa F *et al.* Distinct structural requirements for binding of the integrins alphavbeta6, alphavbeta3, alphavbeta5, alpha5beta1 and alpha9beta1 to osteopontin. *Matrix Biol* 2005; **24**: 418–427.
30. Beshensky AM, Wesson JA, Worcester EM *et al.* Effects of urinary macromolecules on hydroxyapatite crystal formation. *J Am Soc Nephrol* 2001; **12**: 2108–2116.
31. Wesson JA, Ganne V, Beshensky AM *et al.* Regulation by macromolecules of calcium oxalate crystal aggregation in stone formers. *Urol Res* 2005; **33**: 206–212.
32. Wesson JA, Johnson RJ, Mazzali M *et al.* Osteopontin is a critical inhibitor of calcium oxalate crystal formation and retention in renal tubules. *J Am Soc Nephrol* 2003; **14**: 139–147.
33. Junaid A, Amara FM. Osteopontin: correlation with interstitial fibrosis in human diabetic kidney and PI3-kinase-mediated enhancement of expression by glucose in human proximal tubular epithelial cells. *Histopathology* 2004; **44**: 136–146.
34. Kramer AB, Ricardo SD, Kelly DJ *et al.* Modulation of osteopontin in proteinuria-induced renal interstitial fibrosis. *J Pathol* 2005; **207**: 483–492.
35. Ziyadeh FN, Goldfarb S. The renal tubulointerstitium in diabetes mellitus. *Kidney Int* 1991; **39**: 464–475.
36. Pistrosch F, Herbrig K, Kindel B *et al.* Rosiglitazone improves glomerular hyperfiltration, renal endothelial dysfunction, and microalbuminuria of incipient diabetic nephropathy in patients. *Diabetes* 2005; **54**: 2206–2211.
37. Kanjanabuch T, Ma LJ, Chen J *et al.* PPAR-gamma agonist protects podocytes from injury. *Kidney Int* 2007; **71**: 1232–1239.
38. Gassler N, Elger M, Kranzlin B *et al.* Podocyte injury underlies the progression of focal segmental glomerulosclerosis in the fa/fa Zucker rat. *Kidney Int* 2001; **60**: 106–116.
39. Shankland SJ. The podocyte's response to injury: role in proteinuria and glomerulosclerosis. *Kidney Int* 2006; **69**: 2131–2147.
40. Wharram BL, Goyal M, Wiggins JE *et al.* Podocyte depletion causes glomerulosclerosis: diphtheria toxin-induced podocyte depletion in rats expressing human diphtheria toxin receptor transgene. *J Am Soc Nephrol* 2005; **16**: 2941–2952.
41. Roth M, Black JL. Transcription factors in asthma: are transcription factors a new target for asthma therapy? *Curr Drug Targets* 2006; **7**: 589–595.
42. Pascual G, Fong AL, Ogawa S *et al.* A SUMOylation-dependent pathway mediates transrepression of inflammatory response genes by PPAR-gamma. *Nature* 2005; **437**: 759–763.
43. Bidder M, Shao JS, Charlton-Kachigian N *et al.* Osteopontin transcription in aortic vascular smooth muscle cells is controlled by glucose-regulated upstream stimulatory factor and activator protein-1 activities. *J Biol Chem* 2002; **277**: 44485–44496.
44. Renault MA, Jalvy S, Belloc I *et al.* AP-1 is involved in UTP-induced osteopontin expression in arterial smooth muscle cells. *Circ Res* 2003; **93**: 674–681.
45. Sakata R, Minami S, Sowa Y *et al.* Trichostatin A activates the osteopontin gene promoter through AP1 site. *Biochem Biophys Res Commun* 2004; **315**: 959–963.
46. Brosius III FC. Trophic factors and cytokines in early diabetic glomerulopathy. *Exp Diabesity Res* 2003; **4**: 225–233.
47. Nerurkar SS, Olzinski AR, Frazier KS *et al.* P38 MAPK inhibitors suppress biomarkers of hypertension end-organ damage, osteopontin and plasminogen activator inhibitor-1. *Biomarkers* 2007; **12**: 87–112.
48. Ophascharoensuk V, Giachelli CM, Gordon K *et al.* Obstructive uropathy in the mouse: role of osteopontin in interstitial fibrosis and apoptosis. *Kidney Int* 1999; **56**: 571–580.
49. Mazzali M, Hughes J, Dantas M *et al.* Effects of cyclosporine in osteopontin null mice. *Kidney Int* 2002; **62**: 78–85.
50. Chow FY, Nikolic-Paterson DJ, Ma FY *et al.* Monocyte chemoattractant protein-1-induced tissue inflammation is critical for the development of renal injury but not type 2 diabetes in obese db/db mice. *Diabetologia* 2007; **50**: 471–480.
51. Chow FY, Nikolic-Paterson DJ, Ozols E *et al.* Monocyte chemoattractant protein-1 promotes the development of diabetic renal injury in streptozotocin-treated mice. *Kidney Int* 2006; **69**: 73–80.
52. Kato S, Luyckx VA, Ots M *et al.* Renin-angiotensin blockade lowers MCP-1 expression in diabetic rats. *Kidney Int* 1999; **56**: 1037–1048.
53. Collins AR, Schnee J, Wang W *et al.* Osteopontin modulates angiotensin II-induced fibrosis in the intact murine heart. *J Am Coll Cardiol* 2004; **43**: 1698–1705.
54. Neves MF, Amiri F, Virdis A *et al.* Role of aldosterone in angiotensin II-induced cardiac and aortic inflammation, fibrosis, and hypertrophy. *Can J Physiol Pharmacol* 2005; **83**: 999–1006.
55. Sun Y, Zhang J, Lu L *et al.* Tissue angiotensin II in the regulation of inflammatory and fibrogenic components of repair in the rat heart. *J Lab Clin Med* 2004; **143**: 41–51.
56. Eng E, Floege J, Young BA *et al.* Is mesangial cell proliferation required for extracellular matrix expansion in glomerular disease? *Contrib Nephrol* 1994; **107**: 156–162.
57. Young BA, Johnson RJ, Alpers CE *et al.* Cellular events in the evolution of experimental diabetic nephropathy. *Kidney Int* 1995; **47**: 935–944.

58. Brennan BJ, Martin NE. Eplerenone: selective aldosterone antagonism in management of cardiovascular and renal disease. *J Am Pharm Assoc (2003)* 2004; **44**: 604–610; quiz 610–601.
59. Bruemmer D, Collins AR, Noh G *et al.* Angiotensin II-accelerated atherosclerosis and aneurysm formation is attenuated in osteopontin-deficient mice. *J Clin Invest* 2003; **112**: 1318–1331.
60. Liaw L, Birk DE, Ballas CB *et al.* Altered wound healing in mice lacking a functional osteopontin gene (spp1). *J Clin Invest* 1998; **101**: 1468–1478.
61. Potier M, L'Azou B, Cambar J. Isolated glomeruli and cultured mesangial cells as *in vitro* models to study immunosuppressive agents. *Cell Biol Toxicol* 1996; **12**: 263–270.